BATCH AND FIXED BED ADSORPTION STUDIES OF LEAD (II) CATIONS FROM AQUEOUS SOLUTIONS ONTO GRANULAR ACTIVATED CARBON DERIVED FROM *MANGOSTANA GARCINIA* SHELL

Zaira Zaman Chowdhury,[a,]*Sharifuddin Mohd. Zain,[a] Rashid Atta Khan,[a] Rahman Faizur Rafique,[b] and Khalisanni Khalid[c]

The feasibility of granular activated carbon (GAC) derived from Mangostene (*Mangostana garcinia*) fruit shell to remove lead, Pb^{2+} cations was investigated in batch and fixed bed sorption systems. Batch experiments were carried out to study equilibrium isotherms, kinetics, and thermodynamics by using an initial lead (Pb^{2+} ions) concentration of 50 to 100 mg/L at pH 5.5. Equilibrium data were fitted using Langmuir, Freundlich, and Temkin linear equation models at temperatures 30°C, 50°C, and 70°C. Langmuir maximum monolayer sorption capacity was 25.00 mg/g at 30°C. The experimental data were best represented by pseudo-second-order and Elovich models. The sorption process was found to be feasible, endothermic, and spontaneous. In column experiments, the effects of initial cation concentration (50 mg/L, 70 mg/L, and 100 mg/L), bed height (4.5 cm and 3 cm), and flow rate (1 mL/min and 3 mL/min) on the breakthrough characteristics were evaluated. Breakthrough curves were further analyzed by using Thomas and Yoon Nelson models to study column dynamics. The column was regenerated and reused consecutively for four cycles. The result demonstrated that the prepared activated carbon was suitable for removal of Pb^{2+} from synthetic aqueous solution using batch, as well as fixed bed sorption systems.

Keywords: Biomass; Adsorption; Equilibrium; Isotherms; Kinetics; Thermodynamics; Fixed bed

Contact information: a: Department of Chemistry, Faculty of Science, University Malaya, Kuala Lumpur 50603, Malaysia; b: Department of Civil and Environmental Engineering, Kumoh National Institute of Technology (KIT), Gumi, South Korea; c: Malaysian Agricultural Research and Development Institute (MARDI), Selangor, Malaysia
**Corresponding author: zaira.chowdhury76@gmail.com, zaira_chowdhury@live.com*

INTRODUCTION

The presence of metallic contaminants in aqueous effluents emanating from different industries is currently one of the most crucial environmental issues being scrutinized. The addition of heavy metals into the environment affects aquatic life, human health, and the overall ecosystem adversely due to their non-biodegradability, complex state of existence, and very low concentration in a large volume of surface water (Aklil *et al.* 2004; Srivastava and Hasan 2011; Tofan *et al.* 2011). Different metals such as lead (Pb), copper (Cu), manganese (Mn), mercury (Hg), arsenic (As), and zinc (Zn), among others, are known to be highly toxic (Ahluwalia and Goyal 2007).

Among the heavy metals, divalent cations of lead (Pb^{2+} ions) are considered as a priority pollutant (Abdel-Halim *et al.* 2003). Many industries, especially acid battery manufacturing, ceramic and glass industries, ammunition, metal plating, and finishing discharge lead-contaminated water without sufficient treatment to the environment. Even at low concentration, lead can damage the kidneys, nervous system, and reproductive system of people. The Environmental Protection Agency (EPA) has allowed a maximum permissible limit for lead concentration of 0.05 mg/L in waste water (Goel *et al.* 2005). For remediation of lead contamination in waste streams, several methods including precipitation, pH adjustment with alkali hydroxide or lime, ion exchange, reverse osmosis, and coagulation-sedimentation can be utilized (Pan *et al.* 2005; Kobya *et al.* 2005). It has been reported earlier that the precipitation or alkali complexation process produces toxic sludge and is less efficient in diminishing the pollutants concentration to a satisfactory level (Goel *et al.* 2005).

Adsorption by using agricultural biomass can be regarded as one of the most popular methods for the removal of heavy metals including Pb^{2+} from the wastewater due to its abundant availability, biodegradability, and high removal efficiency (Zuorro and Lavecchia 2010; Chowdhury *et al.* 2011a). But the applicability of these materials has been found to be restricted up to a certain extent owing to their small surface area and leaching of some organic substances into the aqueous solution. To overcome such problems, a physio-chemical activation method to produce granular-activated carbon from waste biomass of mangostene fruit shell and thereby enhance its uptake capacity has been undertaken. Adsorption properties of numerous waste biomass such as coconut shell (Sekar *et al.* 2004), tea waste (Amarasinghe and Williams 2007), *Zea mays* (Zvinowanda *et al.* 2010), *Spirogyra neglecta* (Modher *et al.* 2009), oil palm ash (Chowdhury *et al.* 2011a), modified lignin (Demirabas 2004), and rice husk (Wong *et al.* 2003) have been reported for the removal of lead from waste water.

The present research aims to remove Pb^{2+} from synthetic waste water by using mangostene fruit shell based activated carbon (MFSAC), and to investigate the influence of all the physicochemical parameters involved during the batch adsorption process. Textural characteristics of the prepared activated carbon are determined to have insight about the sorption mechanism. The research focuses on adsorption isotherm, kinetics, and thermodynamic characteristics of the prepared adsorbate-adsorbent system. Further information on the efficiency of the prepared activated carbon for continuous flow adsorption has been gathered to study the fixed bed sorption system.The characteristics of the breakthrough curve has been analyzed to ascertain the practical applicability of the adsorbent for fixed bed sorption system.

EXPERIMENTAL

Preparation of Granular Activated Carbon

Raw mangostene fruit shells were collected from the local market of Malaysia. The shells were washed with hot distilled water to remove dust-like impurities and inorganic matters from the surface. After washing, the shells were dried at 105°C for 24 hours to remove moisture content. The dried samples were easy to cut into small pieces

and were sieved to the size of 2 to 3 mm. Granular-activated carbon was prepared by using a two-step physiochemical activation method from the dried sample. Dried fruit shells (50 grams) were placed inside a tubular reactor. The flow rate of purified nitrogen gas and the heating rate were maintained at 150 cm^3/min and 10°C/min, respectively. The temperature was increased from room temperature to 400°C and held constant for 2 hours to carry out the semi-carbonization step. The char produced after semi-carbonization was mixed up with a precise amount of KOH pellets to maintain a ratio 1:1. Deionized water (250 mL) was added to the mixture of char and KOH in a 500 mL beaker with occasional stirring to ensure sufficient mixing of char with KOH and to dissolve all the KOH pellets. The mixture was dried in an oven. Finally, it was activated under CO_2 gas at a flow rate of 150 cm^3/min. The temperature was increased slowly from room temperature and kept constant at 750°C for 2 hours. The prepared activated carbon was washed with hot deionized water several times until the pH range was 6 to 7. The final product (MFSAC) thus obtained was dried and stored in an air-tight container for further application in batch and fixed bed sorption systems.

Physiochemical Characterization of the Granular Activated Carbon

Surface area, volume of the pore, and pore diameter of the prepared activated carbon adsorbent (MFSAC) were measured by Quantachrome Autosorb1, an automated gas sorption system. The average bulk density was determined by water displacement of a definite amount of activated carbon. Thermal Gravimetric analysis was carried out using TGA equipment (Model Perkin Elmer TGA7, US) to investigate the presence of elements of moisture, volatile matters, fixed carbon, and ash residues of the activated carbon.

Preparation of Adsorbate Solution

Stock solution of Pb^{2+} adsorbate was prepared by dissolving 1.6 grams of Pb $(NO_3)_2$, in a 1000 mL volumetric flask followed by dilution up to the mark by addition of de-ionized water. The concentration of lead in the stock solution was 1000 mg/L. The test solutions having concentration of 50 mg/L, 60 mg/L, 70 mg/L, 80 mg/L, 90 mg/L and 100 mg/L were prepared through fresh dilution of the stock solution prior to each adsorption study. The initial pH was adjusted to 5.5 by adding analytical grade dilute hydrochloric acid or sodium hydroxide solution using a pH meter (Mettles Toledo, Model: Ross FE 20, USA).

Batch Adsorption Studies

The batch experiment was carried out by adding 0.2 grams of activated carbon with 50 mg/L, 60 mg/L, 70 mg/L, 80 mg/L, 90 mg/L, and 100 mg/L solution of Pb^{2+} ions. The mixture was agitated at a speed of about 150 rpm until equilibrium was reached in a water bath shaker at a temperature of 30°C, 50°C, and 70°C. The remaining concentration of the cations was analyzed after a set interval of time until equilibrium by using an atomic absorption spectrophotometer (PerkinElmer Model 3100). The amount of Pb^{2+} ion adsorption at equilibrium, q_e (mg/g), was calculated using Equation 1 for a batch sorption system.

$$q_e = \frac{(C_0 - C_e)V}{W} \quad (1)$$

In this expression, q_e (mg/g) is the amount of ion adsorbed at equilibrium. C_o and C_e (mg/L) are the liquid-phase concentrations of Pb^{2+} ions at initial and equilibrium conditions, respectively. V (L) is the volume of the solution, and W (g) is the mass of activated carbon used.

Fixed Bed Adsorption Studies

Fixed bed adsorption studies were conducted in a column made of pyrex glass having an inner diameter of 4.5 cm and a height of 25 cm. A sieve made up of stainless steel was placed at the bottom of the column. Over the sieve, a layer of glass wool was placed to prevent loss of adsorbent. A peristaltic pump (Model Masterfiex, Cole-Parmer Instrument Co., US) was used to pump the feed upward through the column at a desired flow rate. The influent solution was pumped upward to prevent channeling due to gravity. Column dynamics were studied at different conditions of influent concentration, bed height, and flow rate. To determine the effect of concentration on the breakthrough characteristics, 50 mg/L, 70 mg/L, and 100 mg/L inlet concentrations of Pb^{2+}cations were passed through the column at 4.5 bed height using flow rate of 1 mL/min. However, 4.5 cm and 3 cm bed height and 1 mL/min and 3 mL/min flow rates were used to analyze the breakthrough curves using the highest concentration of 100 mg/L.

Column Regeneration Studies

Column regeneration was carried out by using 1M HNO_3 acid solution at flow rate 3 mL/min, slightly higher than the influent flow rate to provide sufficient exchangeable H^+ ions for 16 hours. After each cycle, the adsorbent was washed with hot distilled water and then packed inside the column. The regeneration efficiency (RE%) was calculated for a bed height of 4.5 cm, flow rate of 1 mL/min, and initial concentration of 100 mg/L.

RESULTS AND DISCUSSION

Physiochemical Characterization of the Granular Activated Carbon

The adsorption performance of the activated adsorbent is highly influenced by its physical and chemical properties. The surface area, pore volume, and diameter with other physiochemical characteristics of the semi-carbonized char and prepared activated carbon are listed in Table 1. It was observed that, after the activation process, BET surface area and total pore volume increased significantly. This might be due to involvement of both chemical and physical activating agents of KOH and CO_2, respectively, during the activation process. However, KOH is acting here as a strong dehydrating agent. During activation at a higher temperature, it can produce K_2O which can further react with CO_2 to yield K_2CO_3 by water shift reaction (Salman and Hameed 2010). Thus, intercalation of metallic potassium inside the carbon matrix of the char caused drastic expansion of surface area, pore volume, and diameter of the prepared activated carbon (MFSAC).

According to IUPAC classification the prepared sorbent is of mesoporous type (IUPAC Manual 1982).

Table 1. Physio-Chemical Characteristics of Raw Fruit Shell and Granular Activated Carbon (MFSAC) for Sorption of Pb (II) Cations

Physio-Chemical Characteristics	Semi-Carbonized Char	Granular Activated Carbon (MFSAC)
BET surface area	1.034 m^2/g	312.03 m^2/g
Micropore Surface area (DR method)	1.434 m^2/g	261.3 m^2/g
Total pore volume (DR method)	0.0051 cc/g	0.128 cm^3/g
Average pore diameter	4.087 °A	28.9° A
Cumulative adsorption surface area (BJH method)	1.66 m^2/g	178.3 m^2/g
Bulk density	-	0.435 g/mL
Moisture	4.78	3.33
Volatile Matter	72.88	32.66
Fixed Carbon	18.80	54.02
Ash	3.54	9.99

The chemical characteristics of the char along with the activated carbon were analyzed by TGA analysis and listed in Table 1. From Table 1, it was observed that the fixed carbon content increased while the volatile matter decreased significantly after activation of the char. The bulk density of the prepared sorbent (MFSAC) obtained was 0.435 g/cm^3.

Batch Adsorption Studies

Effects of contact time and concentration

The effects of the initial metal ion concentration in the range of 50 mg/L to 100 mg/L for sorption were investigated with respect to contact time and are illustrated in Fig. 1. It is evident that the equilibrium uptake, q_t (mg/g), of Pb^{2+} increased proportionally with the initial concentration of the solution. The increase in initial concentration enhances the interaction between Pb^{2+} and active sites of MFSAC. Higher concentration provides a relatively large driving force to overcome the resistance to the mass transfer of the sorbate between solid and liquid phase, resulting in a greater uptake capacity. However, percentage removal of Pb^{2+} showed an opposite trend. As the concentration increased, the removal percentage decreased. The percentage of Pb^{2+} removal was found to be 85.82 % for the 50 mg/L sample while 71.45 % was found for the 100 mg/L solution at 30°C. The adsorption was very fast at the beginning until 60 minutes. With increasing time, the sorption rate became more or less stable for all the concentration ranges, being studied until the system reached equilibrium at 60 minutes. The rapid rate of sorption at the initial stage is due to the increased concentration gradient between the presence of Pb^{2+} in liquid phase and onto the solid surface of MFSAC. At the initial stage, there were a large number of vacant active sites which were progressively occupied by Pb^{2+}cations. With the lapse of time, when the system was approaching equilibrium, the uptake rate was slower (Amarasinghe and Williams 2007; Srivastava and Hasan 2011).

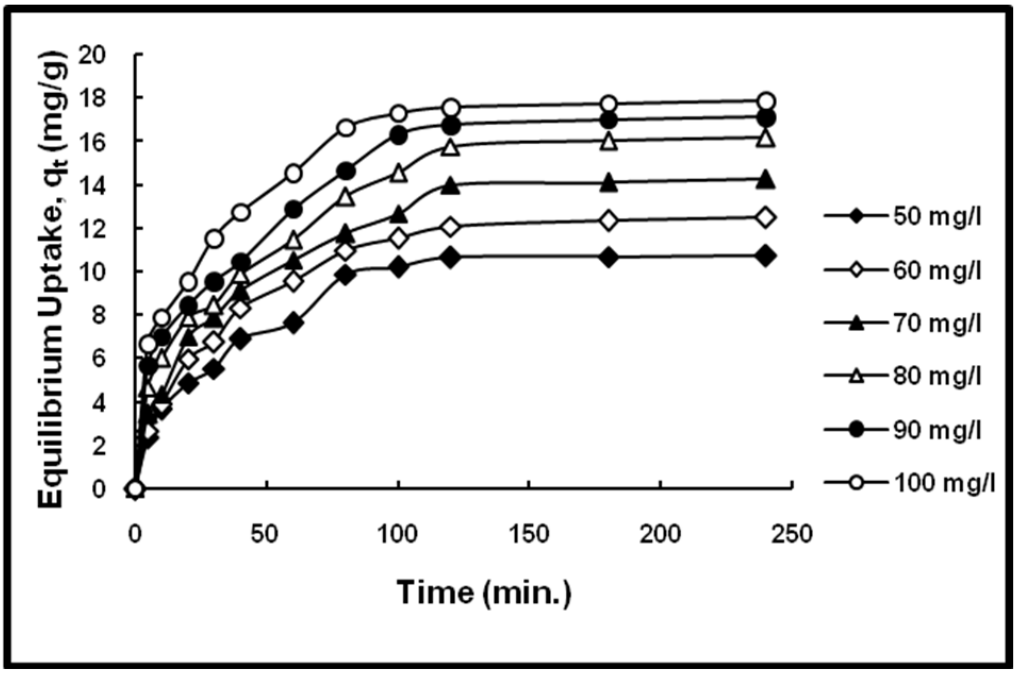

Fig. 1. Effect of initial metal ion concentration and contact time (min.): C_0 = 50 mg/L to 100 mg/L, Temperature = 30 °C, pH = 5.5

Equilibrium kinetics studies

The kinetics of adsorption describes the rate of adsorbate uptake (Pb^{2+}) on the adsorbent at a predetermined interval and equilibrium contact time. The kinetic parameters are essential for the calculation of adsorption rate, providing significant information for designing and modeling the full scale batch process (Kalavathy *et al.* 2005).

The pseudo-first-order kinetic model has been widely used to predict sorption kinetics (Srivastava and Hasan 2011). The model is defined by Equations (2) and (3),

$$\log(q_e - q_t) = \log q_e - \frac{k_1}{2.303} t \quad (2)$$

$$h = k_1 q_{e_{cal}} \quad (3)$$

where, q_e and q_t are the amounts of adsorbate adsorbed (mg/g) at equilibrium and at time t (minute) respectively, h (mg/g-min) is the initial rate of sorption, and k_1 (min^{-1}) is the adsorption rate constant. Figure 2 illustrates the linear plots of ln (q_e-q_t) versus t (minutes) for all the concentrations being studied. First order rate constant k_1, and theoretical uptake, q_e (mg/g) were calculated from the slope and intercepts and listed in Table 2.

The linear form of pseudo-second-order equation based on equilibrium

adsorption is expressed by (Ho and McKay, 1998) Equations (4) and (5),

$$\frac{t}{q_t} = \frac{1}{k_2 q_e^{\ 2}} + \frac{1}{q_e} t \quad (4)$$

$$h = k_2 q_{e_{cal}}^2 \quad (5)$$

where k_2 (g/mg-min) is the rate constant of second-order adsorption and h (mg/g-min) is the initial rate of sorption. The linear plots of t/q_t, versus t (mins.) gives $1/q_e$ as the slope and $1/k_2q_e$ as the intercept and is shown by following Fig. 3.

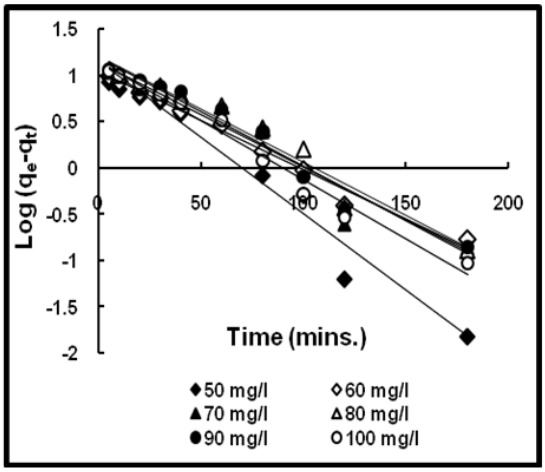

Fig. 2. Pseudo-First-Order Plots: C_0 = 50 mg/l-100 mg/l, Temperature = 30°C and pH = 5.5

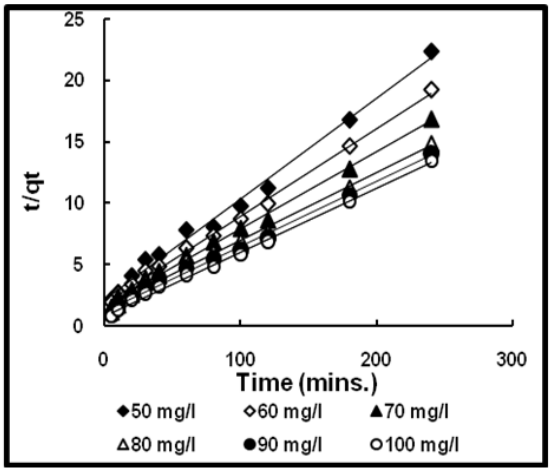

Fig. 3. Pseudo-Second-Order Plots: C_0 = 50 mg/l-100 mg/l, Temperature = 30°C and pH =5.5

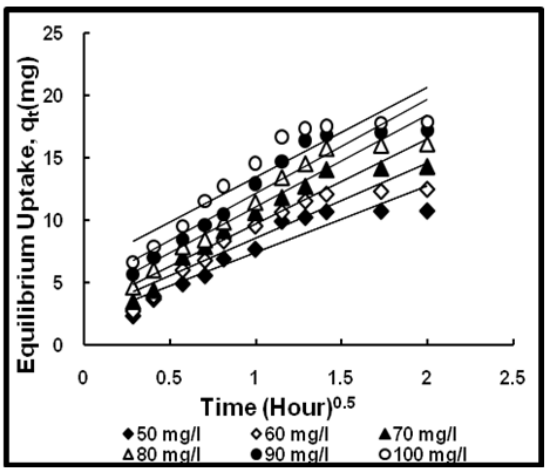

Fig. 4. Intra-particle Diffusion Plots: C_0 = 50 mg/l-100 mg/l, Temperature = 30°C, and pH = 5.5

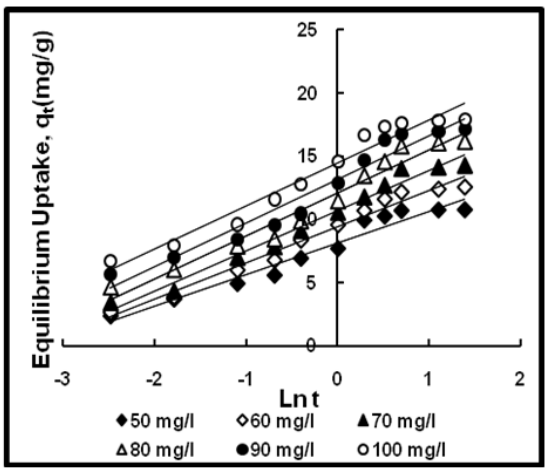

Fig. 5. Elovich Equation Plots: C_0= 50 mg/l-100 mg/l, Temperature = 30°C, and pH =5

Based on relatively low coefficients of correlation and large differences between experimental and calculated equilibrium uptake capacity, it was observed that pseudo-first-order kinetics was not applicable for the system under investigation. In contrast, pseudo-second-order plots (Fig. 3) showed good linearity independent of concentration range when compared to pseudo-first-order plots. The calculated uptake capacities from pseudo-second-order kinetics model agreed very well with the experimental data with high correlation coefficients. Both facts suggested that the adsorption of Pb^{+2} cations by MFSAC followed pseudo-second-order kinetics, reflecting that chemisorptions might be the rate-limiting step in the sorption process.

Table 2. Comparison of Pseudo-First-Order and Pseudo-Second-Order Adsorption Rate Constant for Different Initial Concentration at 30 °C Temperature

	Pseudo First Order					Pseudo Second Order			
C_0 (mg/L)	$q_{e,(exp)}$ (mg/g)	$q_{e,(cal)}$ (mg/g)	k_1 (min^{-1})	h	R^2	$q_{e,(cal)}$ (mg/g)	k_2 (min^{-1})	h	R^2
50	10.7275	14.2889	0.0368	0.526	0.956	12.0481	0.0035	0.502	0.996
60	12.5050	10.9647	0.0230	0.252	0.985	14.0845	0.0028	0.545	0.997
70	14.2550	13.9312	0.0253	0.352	0.941	16.1290	0.0022	0.580	0.995
80	16.1650	16.1065	0.0276	0.445	0.960	18.5185	0.0017	0.593	0.980
90	17.1432	15.6315	0.0299	0.467	0.968	19.2307	0.0023	0.847	0.991
100	17.8603	14.0928	0.0322	0.454	0.980	19.6078	0.0023	0.888	0.989

The intraparticle diffusion model is used to test the role of diffusion as the rate-limiting step in the adsorption process and is defined by Equation 6 (Kalavathy *et al.* 2005),

$$q_t = K_{id} t^{0.5} \quad (6)$$

where, K_{id} (mg/g h) is the intraparticle diffusion rate constant obtained from the slope of the straight line of q_t (mg/g) versus $t^{0.5}$(hour), and C is obtained from intercepts. The value of C gives an idea about the thickness of the boundary layer (Kannan and Sundaram 2001). Figure 4 shows the intraparticle diffusion plots, and the model parameters are listed in Table 3.

Table 3. Intraparticle Diffusion Model Rate Constant for Different Initial Concentration at 30 °C Temperature

Initial Concentration (mg/L)	C	K_{dif} (mg/gh$^{0.5}$)	R^2	$q_{e,cal}$ (mg/g)
50	2.491	5.147	0.838	12.785
60	2.498	6.053	0.883	14.604
70	2.644	6.943	0.903	16.530
80	3.171	7.422	0.939	18.051
90	4.496	7.648	0.902	19.792
100	4.986	7.611	0.891	20.208

Two regions were observed here for intraparticle diffusion plots (Fig. 4). At the initial stage, a sharper region was observed due to the instantaneous adsorption or external surface adsorption process. The second region was the gradual adsorption stage where intraparticle diffusion was the rate-limiting step. The straight lines deviated from the origin, indicating that pore diffusion, as well as other mechanisms were involved in the rate-controlling step (Mall *et al.* 2006).

The Elovich equation was further implemented for analyzing the experimental data to elucidate the chemisorption nature of the equilibrium system under investigation as seen by Equation 7,

$$q_t = \frac{1}{b} Ln(ab) + \frac{1}{b} Lnt \quad (7)$$

where a (mg/g-h) represents initial sorption rate, and b (g/mg) depicts activation energy and extent of surface coverage for chemisorption. The value of $1/b\ Ln\ (ab)$ is the sorption quantity when t (time) equals to zero, that is t is 1 hour; whereas $1/b$ indicates the number of sorption sites for binding. The linear plots of the Elovich model are shown in Fig. 5, and the model parameters are listed in Table 4. The good linearity showed by the lines in Fig. 5 and high correlation coefficients further support chemisorption nature of adsorption process.

Table 4. Elovich Model Rate Constant for Different Initial Concentration at 30 °C Temperature

Initial Concentration (mg/L)	1/*b*	1/*b* ln (*ab*)	R^2	$q_{e,cal}$ (mg/g)
50	2.473	8.420	0.958	11.848
60	2.862	9.409	0.977	13.376
70	3.234	10.56	0.969	15.043
80	3.319	11.61	0.929	16.211
90	3.517	13.21	0.944	18.085
100	3.467	13.65	0.915	18.456

Equilibrium Isotherm Studies

Adsorption isotherms provide elementary physiochemical statistics for describing the distribution of adsorbate between solid and liquid phases for a specific adsorbent-adsorbate system under fixed reaction condition. The results obtained in this study were fitted with well known Langmuir, Freundlich, and Temkin isotherm models.

Langmuir model was originally developed for adsorption of gases onto the solid adsorbent and is also known as an ideal localized monolayer model (Langmuir 1918). The Langmuir model is expressed as Equation 8.

$$q_e = \frac{q_m K_L C_e}{1 + K_L C_e} \quad (8)$$

The linear form of the Langmuir isotherm equation can be written as Equation 9,

$$\frac{C_e}{q_e} = \frac{1}{q_m K_L} + \frac{1}{q_m} C_e \quad (9)$$

where C_e is the equilibrium concentration of the adsorbate (mg/L), q_e is the amount of adsorbate adsorbed per unit mass of adsorbent (mg/g), and q_m (mg/g) and K_L (L/mg) are the Langmuir constants related to the maximum monolayer adsorption capacity and rate of adsorption, respectively. When C_e/q_e is plotted against C_e, a straight line with a slope of $1/q_m$ and intercept of $1/q_m K_L$ is obtained (figure not shown). The essential term of the Langmuir isotherm or separation factor, R_L is represented by Equation 10,

$$R_L = \frac{1}{1 + K_L C_0} \quad (10)$$

where, C_0 is the adsorbate highest initial concentration (100 mg/L). Langmuir separation factor R_L is a dimensionless constant which is described by Table 5 (Chowdhury *et al.* 2012).

Table 5. Description of Langmuir Constant R_L

Values of R_L	Types of Isotherm
$R_L > 1$	Unfavorable
$R_L = 1$	Linear
$0 < R_L < 1$	Favorable
$R_L = 0$	Irreversible

The Freundlich model is an empirical equation that encompasses the heterogeneity of the surface or surface sustaining sites of wide-ranging affinities (Chowdhury *et al.* 2011b). It is based on exponential distribution of active sites and their energies. The Freundlich isotherm (Freundlich 1906) is expressed by Equation 11.

$$q_e = K_F C_e^{1/n} \quad (11)$$

The well-known logarithmic form of Freundlich isotherm is given by Equation 12.

$$Lnq_e = LnK_F + \frac{1}{n} LnC_e \quad (12)$$

Here, C_e (mg/L) is the equilibrium concentration of the adsorbate, q_e (mg/g) is the amount of adsorbate adsorbed per unit mass of adsorbent (mg/g), and K_F and n are Freundlich constants. K_F (mg/g (L/mg)) can be defined as the adsorption or distribution coefficient and represents the quantity of adsorbate adsorbed onto the adsorbent for a unit equilibrium concentration, and n represents the intensity factor of sorption.

The Temkin isotherm is based on a factor that explicitly takes into account the adsorbent-adsorbate interactions (Temkin and Pyzhev 1940). This model assumes that the heat of adsorption of all the molecules in the layer would decrease linearly with coverage due to adsorbent-adsorbate interactions. The adsorption is characterized by a regular distribution of binding energies, up to some maximum binding energy. The Temkin model is expressed as:

$$q_e = (\frac{RT}{b}) Ln(K_T C_e) \quad (13)$$

The linear form of Temkin Isotherm is

$$q_e = BLnK_T + BLnC_e \quad (14)$$

$$B = \frac{RT}{b} \quad (15)$$

Here, R is the gas constant (8.314 J/mol K), T is the absolute temperature (°K), and $RT/b=B$. A plot of q_e versus in LnC_e yields a linear line with B as the slope and B ($\ln K_T$)

as the intercept (Figure not shown). K_T (L/g) represents the equilibrium binding constant, and *B* is a heat related constant. However, the isotherm model parameters were evaluated at 30°C, 50°C, and 70°C to study the effect of temperature on the sorption process. The model parameters are provided in Table 6.

Table 6. Isotherm Model Parameters at 30 °C, 50 °C, and 70 °C Temperature

Temp. (°C)	Langmuir Isotherm				Freundlich Isotherm			Temkin Isotherm		
	q_{max} (mg/g)	K_L (L/mg)	R_L	R^2	K_F (mg/g)(L/mg)$^{1/n}$	1/*n*	R^2	*B*	K_T (L/mg)	R^2
30	25.00	0.1075	0.0066	0.995	5.2593	0.382	0.939	5.428	1.066	0.956
50	27.03	0.1331	0.0064	0.937	6.8757	0.332	0.925	5.014	2.014	0.916
70	27.78	0.1463	0.0054	0.883	7.4558	0.321	0.907	4.921	2.555	0.858

From Table 5, it was observed that the experimental data followed the Langmuir model significantly better than the Freundlich or Temkin isotherm models for all the temperature ranges studied, reflecting the homogeneous nature of MFSAC. It also suggested that the adsorption process of Pb^{2+} onto MFSAC was a monolayer (Pruksathorn and Vitidsant 2009), and adsorption of each cation had equal activation energy. Maximum monolayer sorption capacity, q_m (mg/g) increased with an increase in temperature, demonstrating endothermic nature of sorption. The Langmuir separation factor, R_L values obtained were between 0 to1 for all the temperature indicating that the adsorption process of Pb^{2+} onto MFSAC was favorable. Freundlich exponent, *1/n* ranging between 0 and 1 is a measure of adsorption intensity or surface heterogeneity. A value of *1/n* below one reflects favorable adsorption of Pb^{2+}onto MFSAC (Chowdhury *et al.* 2011a,b; 2012). With the increase in temperature, the values of K_F also increased. The experimental data were further analyzed by Temkin isotherm, which showed a higher regression coefficient, reflecting strong affinity for adsorption of Pb^{2+}onto MFSAC (Kalavathy *et al.* 2005).

Thermodynamics studies

Thermodynamic parameters describing ΔG°, Gibbs free energy, ΔH°, change in enthalpy of reaction, and ΔS°, change in entropy for adsorbate-adsorbent interaction can be calculated by using Equations 16 and 17.

$$\ln K_L = \frac{\Delta S}{R} + \frac{\Delta H}{RT} \quad (16)$$

$$\Delta G = RTLnK_L \quad (17)$$

In these equations, K_L (L/mg) is the Langmuir Isotherm constant at different temperatures; *R* is the universal gas constant (8.314 j/ mol. K), and *T* is absolute

temperature in Kelvin. The values of $\Delta H°$ and $\Delta S°$ can be determined from the linear plot of $\ln K_L$ versus $1/T$ (Figure not shown). However, the values of thermodynamic parameters were determined and listed in Table 7.

Table 7. Thermodynamic Parameters of Pb (II) Sorption onto Granular Activated Carbon (MFSAC)

Temperature,°K	$\Delta G°$(kj-mol^{-1})	$\Delta H°$ (kj-mol^{-1})	$\Delta S°$ (jK^{-1} mol^{-1})	R^2
303	-5.618			
323	-5.416	+6.7085	+3.7165	0.964
343	-5.481			

The enthalpy change obtained here was +6.7085 (kj-mol^{-1}), which was consistent with Langmuir monolayer sorption capacity, q_m (mg/g), reflecting the endothermic nature of sorption. The result was also consistent with a successive increase in Freundlich affinity factor, K_F with an increase of temperature. The positive value of entropy, $\Delta S°$ represented an increase in the degree of freedom of the adsorbate. The positive value of $\Delta S°$ also reflected that some changes took place in the internal structure of MFSAC during the adsorption process. Similar types of observation were reported previously for removal of lead from wastewater by using activated palm ash (Chowdhury *et al.* 2011a). The magnitude of Gibbs free energy change ($\Delta G°$) obtained was negative, demonstrating that the adsorption took place spontaneously for the temperature range being studied. The negative value of ΔG reflected feasibility of sorption.

Fixed Bed Adsorption Studies

Effect of adsorbate inlet concentration

The effect of adsorbate concentration (Pb^{2+} ions) on the column performance was studied by varying the inlet concentration of lead between 50 mg/L, 70 mg/L, and 100 mg/L while the same adsorbent bed height of 4.5 cm and feed flow rate of 1 mL/min were used. The breakthrough curve is illustrated in Fig. 6.

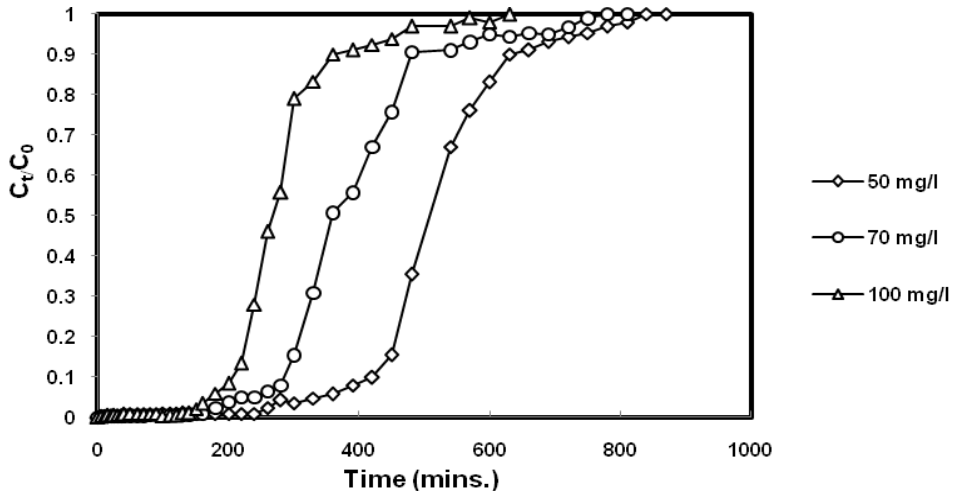

Fig. 6. Breakthrough curves for adsorption of Pb (II) onto MFSAC for different initial concentration (Flow rate 1 mL/min, pH 5.5, Temperature 30 °C)

As can be observed from the plots (Fig. 6), the activated carbon beds were exhausted faster at higher adsorbate inlet concentration for 100 mg/L. That is, an earlier breakthrough point was reached at higher concentration, leading to a relatively steeper curve when compared to the lower concentration. The breakthrough time, t_b (minutes.) was found to decrease with increasing adsorbate inlet concentration as the binding sites became more quickly saturated in the column. A decrease in inlet concentration gave an extended breakthrough curve, indicating that a higher volume of solution could be treated. This is due to the fact that a lower concentration gradient would cause a slower transport resulting in a decrease in diffusion coefficient or mass transfer coefficient (Taty-Costodes *et al.* 2005).

Effect of activated carbon bed height

Figure 7 shows the breakthrough curve obtained for adsorption of Pb^{2+} on MFSAC for two different bed heights of 3 cm and 4.5 cm (3.56 and 4.86g of MFSAC) at constant adsorbate feed flow rate of 1 mL/min and adsorbate inlet concentration of 100 mg/L.

As can be seen from Fig. 7, both the breakthrough time, t_b (minutes) and exhaustion time, t_e (minutes) were found to increase with increasing bed height. The plots indicate the shape and gradient of the breakthrough curves were slightly different with variations in bed depth, which was expected.

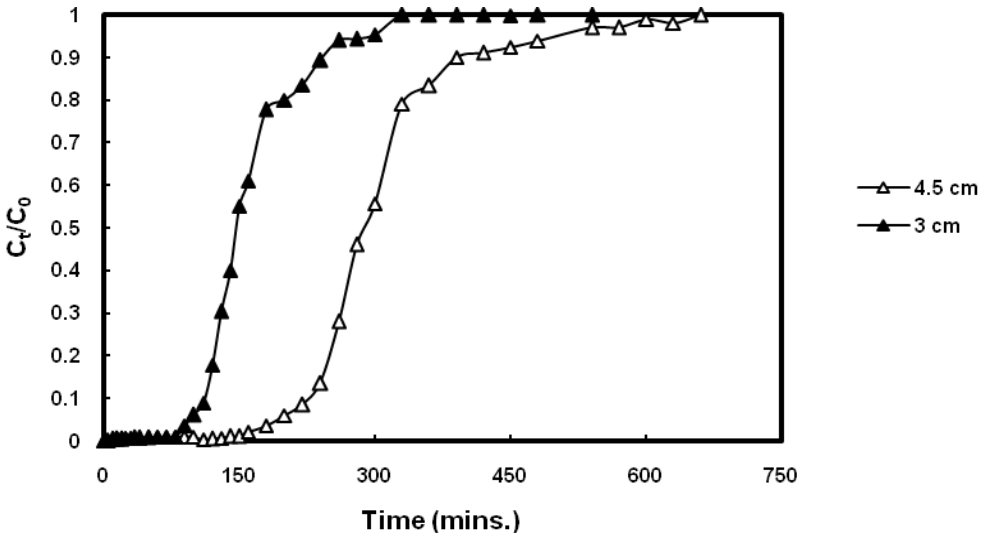

Fig. 7. Breakthrough curves for adsorption of Pb (II) onto MFSAC for different bed height (concentration 100 mg/L, flow rate 1 mL/min, pH 5.5, temperature (30 °C)

A higher uptake was observed at higher bed height due to the increase in the specific surface area of the activated carbon, which provided more fixation of the cations with active binding sites for the adsorption process to proceed. The increase in bed height would increase the mass transfer zone. The mass transfer zone in a column moves from the entrance of the bed and proceeds toward the exit. Hence, for the same influent

concentration and fixed bed system, an increase in bed height would create a longer distance for the mass transfer zone to reach the exit, subsequently resulting in an extended breakthrough time. For higher bed depth, the increase of adsorbent mass would provide a larger service area leading to an increase in the volume of the treated solution (Taty-Costodes *et al.* 2005).

Effect of feed flow rate

The effect of feed flow rate on the adsorption of Pb^{2+}on MFSAC was investigated by varying the feed flow rate (1 and 3 mL/min) at a constant adsorbent bed height of 4.5 cm and inlet adsorbate concentration of 100 mg/L, as shown by the breakthrough curve in Fig. 8. The trend of the curves showed that at higher flow rate, the front of the adsorption zone quickly reached the top of the column. This implies that the column was saturated early. Lower flow rate resulted in longer contact time, as well as a shallow adsorption zone. Higher flow rates are seen by the steeper curve with relatively early breakthrough and exhaustion time; they resulted in less adsorption uptake (Sarin *et al.* 2006).

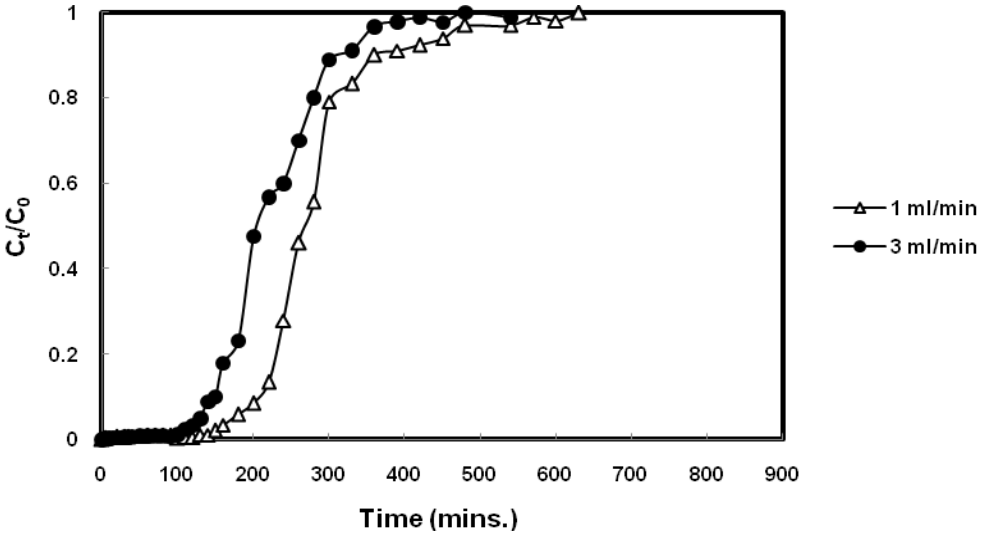

Fig. 8. Breakthrough curves for adsorption of Pb (II) onto MFSAC for different flow rates (concentration 100 mg/L, pH 5.5, temperature (30 °C)

Application of Thomas model

Thomas model is based on the assumption that the process follows Langmuir kinetics of adsorption-desorption with no axial dispersion. It describes that the rate driving force obeys 2nd order reversible reaction kinetics. The linearized form of the model is given by Equation 18 (Chun *et al.* 2009).

$$\ln\left[\left(\frac{C_o}{C_t}\right)-1\right]=\left(\frac{k_{Th}q_o m}{Q}\right)-\left(\frac{k_{Th}q_o V_{eff}}{Q}\right) \quad (18)$$

In this expression k_{Th}, (mL/mg min) is the Thomas rate constant, q_0 (mg/g) is the equilibrium adsorbate uptake, and m is the amount of adsorbent in the column (Thomas 1944).

The experimental data were fitted with the Thomas model to determine the rate constant (k_{th}) and maximum capacity of sorption (q_0). The k_{th} and q_0 values were calculated from the slope and intercepts of linear plots of ln [(C_0/C_t)-1] against t (mins.) using values from the column experiments (Figure not shown). The model parameters are listed in Table 8.

Table 8. Thomas Model Parameters for Pb(II) at Different Conditions using Linear Regression Analysis

Initial Concentration (mg/L)	Bed Height (cm)	Flow Rate (mL/min)	k_{th} (mL/min-mg) x 10^{-4}	q_o (mg/g)	R^2
50	4.5	1	3.80	5523.06	0.986
70	4.5	1	3.00	5617.28	0.980
100	4.5	1	2.60	6702.88	0.976
100	3.0	1	3.10	4721.82	0.922
100	4.5	3	4.70	6435.51	0.864

As the concentration increased, the value of k_{th} decreased, whereas the value of q_o showed a reverse trend, *i.e.*, increased with an increase in concentration. The bed capacity (q_o) increased and the coefficient (k_{th}) decreased with an increase in bed height. Similarly, q_o values decreased and k_{th} values increased with an increase in the flow rate. A similar trend has also been observed for sorption of Cr(VI) by activated weed-fixed bed column (Baral *et al.* 2009) and azo dye removal onto bamboo-based activated carbon (Ahmad and Hameed 2010). Experimental data fitted the Thomas model, indicating that the external and internal diffusion is not the limiting step, and no axial dispersion is present.

Application of the Yoon-Nelson model

A simple theoretical model developed by Yoon-Nelson was applied to investigate the breakthrough behavior of Pb^{2+} ions on MFSAC. The linearized model for a single component system is expressed by Equation 19,

$$\ln\left[\frac{C_t}{C_o - C_t}\right] = k_{YN}t - \tau k_{YN} \quad (19)$$

where k_{YN} (min^{-t}) is the rate constant and τ is the time required for 50% adsorbate breakthrough (Yoon and Nelson 1984).

Table 9. Yoon-Nelson Model Parameters for Pb (II) at Different Conditions using Linear Regression Analysis

Initial Concentration (mg/l)	Bed Height (cm)	Flow Rate (ml/min)	k_{YN} (l/min)	ζ (min)	R^2
50	4.5	1	0.020	536.84	0.986
70	4.5	1	0.021	382.38	0.980
100	4.5	1	0.029	280.82	0.976
100	3.0	1	0.031	168.09	0.922
100	4.5	3	0.026	103.44	0.815

The values of k_{YN} and τ were estimated from slope and intercepts of the linear graph between ln $[C_t/(C_o - C_t)]$ versus t (mins.) at different flow rates, bed heights, and initial cation concentration (Figures are not shown). From Table 8, it was observed that values of k_{YN} were found to decrease with increases in bed height, and the corresponding values of τ increased with increasing bed height. With an increase in initial cation concentration, the k_{YN} increased but τ values decreased (Ahmad and Hameed 2010). With an increase in flow rates, the values of k_{YN} and τ decreased. A similar trend was found by Cd (II) on coir pith for column mode sorption (Bharathi *et al.* 2011).

Column Regeneration Studies

MFSAC were tested for four cycles after the initial application, using 1 M HNO_3 as an eluting agent at a flow rate of 3 mL/min for 16 hours. It was observed that the amount of desorption was negligible after 570 minutes.

Based on the Yoon Nelson model, the amount of adsorbate being adsorbed in a fixed bed column is half of total adsorbate entering within 2ζ period (Bharathi *et al.* 2011). Thus, the sorption capacity of a column, q_{org} or q_{eq} (mg/g) is calculated from Equation 20 and tabulated in Table 10 for each cycle.

$$Capacity, q_{eq} = \frac{C_0 r \zeta}{1000m} \quad (20)$$

Here, C_0 is the initial concentration, r is flow rate, and m is mass of the activated carbon in fixed bed. The regeneration efficiency (RE%) was calculated for bed height of 4.5 cm, flow rate 3 mL/min, and initial concentration of 100 mg/L by using Equation 21.

$$RE(\%) = \frac{q_{reg}}{q_{org}} \times 100 \quad (21)$$

However, the breakthrough time, t_b(minutes), complete exhaustion time, t_e(minutes),and regeneration efficiency for different conditions were determined and listed in Table 10.

Table 10. Regeneration of Fixed Bed Column

Adsorbate Cation	Cycle No	Breakthrough Time, t_b (minute)	Column Uptake Capacity (mg/g)	Complete Bed Exhaustion Time, t_e (minute)	Regeneration Efficiency (%)
Lead (II)	1	180	6.7028	630	original
	2	130	5.3243	450	79.43
	3	100	3.5658	180	53.19
	4	70	2.2987	120	34.29

It was found that the fixed bed sorption system performed better at a lower flow rate and concentration of the influent using higher bed height. These observations were in agreement with the research reported previously on various column mode sorption systems (Al-Qodah and Lafi 2003; Padmesh *et al.* 2006; Malkoc *et al.* 2006). Overall, the sorption capacity observed for fixed bed system was lower than the batch system for the same initial concentration. This might be due to the insufficient contact time between the adsorbate and adsorbent in the fixed bed system than the stirred batch vessels (Al-Qodah and Lafi 2003).

CONCLUSIONS

1. The physico-chemical activation technique was used to prepare the adsorbent (MFSAC) from waste biomass of mangostene fruit shell. This approach was successful in creating sufficient porosities and surface area for adsorption of Pb^{2+} from synthetic waste water.
2. Adsorption data fitted the Langmuir model better than the Freundlich and Temkin adsorption isotherm models.
3. Batch equilibrium data followed pseudo-second-order kinetics, and the Elovich equation reflected chemisorption as the rate-controlling step.
4. Equilibrium uptake increased with an increase in temperature, reflecting endothermic nature of sorption which was further confirmed by thermodynamic characterizations of the system.
5. Adsorption capacity determined for 50 mg/L, 70 mg/L, and 100 mg/L feed concentration of Pb^{2+} at different conditions were less than the batch method for the same intial concentration used. This may be caused by the probable irreversibility of the sorption process and the different approaches to adsorption equilibrium in batch and continuous flow systems in column mode sorption.
6. Removal of Pb^{2+} onto the prepared adsorbent (MFSAC) depends on an inlet feed concentration, bed height, and flow rate for fixed bed sorption system.

7. Fixed bed sorption data has shown a good agreement with well established column models, namely the Thomas and Yoon Nelson models.
8. The adsorbed Pb^{2+} ions can be effectively eluted with the use of 1 M HNO_3 acid with the regeneration efficiency of 53.19% up to three cycles. On the basis of batch and bench scale column studies, it can be concluded that the adsorbent (MFSAC) can be used repeatedly without significant loosing of sorption capacity reflecting its feasibility for commercial application.

ACKNOWLEDGMENTS

The authors are grateful for the financial support of this project by Research Grant (UMRG 056-09SUS) of University Malaya, Kumoh National Institute, South Korea (KIT) and Malaysian Agricultural Research and Development Institute (MARDI), Malaysia for their continuous encouragement.

REFERENCES CITED

Abdel-Halim, S. H.,Shehata, A. M. A., and El-Shahat, M. F. (2003). "Removal of lead ions from industrial waste water by different types of natural materials," *Water Res*. 37, 1678-1683.

Ahmad, A. A., and Hameed, B. H. (2010). "Fixed bed adsorption of azo dye onto granular activated carbon from prepared from waste,"*J. Hazard. Mater*.175, 298-203.

Ahluwalia, S. S., and Goyal, D. (2007). "Microbial and plant derived biomass for removal of heavy metals from wastewater,"*Bioresour. Technol*. 98, 2243-2257.

Aklil, A., Moutflih, M., and Sebti, S. (2004). "Removal of heavy metal ions from water by using calcined phosphate as a new adsorbent," *J. Hazard. Mater*. A112, 183-190.

Al-Qodah, Z., and Lafi., W. (2003). "Adsorption of reactive dyes using shale oil ash in fixed beds," *Journal of Water Supply: Research and Technology* 52, 189-198.

Amarasinghe, B. M. W. P. K., and Williams, R. A. (2007), "Tea waste as low cost adsorbent for the removal of Cu and Pb from waste water," *Chem. Eng. J.* 132, 299-309.

Baral, S. S., Das, N., Ramulu, T. S., Sahoo, S. K., Das, S. N., and Chaudhury, G. R. (2009). "Removal of Cr(VI) by thermally activated weed *Salvinia cucullata* in a fixed bed column,"*J. Hazard. Mater.* 161, 1427-1435.

Bharathi, K. S., Badabhagni, N., Nidheesh, P. V., Gandhimathi, R., and Ramesh, S. T. (2011). "Breakthrough data analysis of adsorption of Cd(II) on coir pith column,"*EJEAFChe.*10(8), 2638-2658.

Chowdhury, Z. Z., Zain, S. M., and Rashid, A. K. (2011a). "Equilibrium isotherm modelling, kinetics, and thermodynamics study for removal of lead from waste water," *E. J. Chem*. 8(1), 333-339.

Chowdhury, Z. Z., Zain, S. M., Rashid, A. K., and Ahmed A. A. (2011b). "Equilibrium kinetics and isotherm studies of Cu (II) adsorption from waste water onto Alkali Activated Oil Palm Ash,"*Am. J. Applied Sci.* 8(3), 230-237.

Chowdhury, Z. Z., Zain, S. M., Rashid, A. K., and Islam, M. S. (2012). "Preparation and characterizations of activated carbon from kenaf fiber for equilibrium adsorption studies of copper from wastewater," *Korean J. Chem. Engineering* 1-9.

Chun, Y. Y., Aroua, M. K., and Wan Daud, W. M. A. (2009). "Fixed bed adsorption of metal ions from aqueous solution on polyethylineimine-impregnated palm shell activated carbon," *Chem. Eng. J.* 148, 8-14.

Demirabas, A., (2004). "Adsorption of lead and calcium ions in aqueous solutions onto modified lignin front alkali glycerol delignication," *J. Hazard. Mater*. B109, 221-226.

Freundlich, H. M. F. (1906). "Over adsorption in solution," *J. Phys. Chem.* 57, 385-470.

Goel, J., Kadirvelu, K., Rajagopal, C., and Carg, V. K. (2005). "Removal of Pb(II) by adsorption using treated granular activated carbon: batch and column studies," *J. Hazard.Mater.* B 125, 2l1-210.

Ho, Y. S. (2006). "Review of second order models for adsorption systems," *J. Hazard. Mater.*136, 681-689.

IUPAC Manual of Symbols and Terminology of Colloid Surface, Butterworths, London, 1982, p. 1.

Kalavathy, M. H., Karthikeyan, T., Rajgopal, S., and Miranda, L. R. (2005). "Kinetic and isotherm studies of Cu (II) adsorption onto H_3PO_4- activated rubber wood sawdust," *J. Colloid Interface Sci.* 292, 354-362.

Kannan, K., and Sundaram, M. M. (2001). "Kinetics and mechanism of removal of methylene blue by adsorption on various carbons e a comparative study," *Dyes Pigments* 51, 25-40.

Kobya, M., Demirbas, E., Senturk, E., and Ince, M. (2005). "Absorption of heavy metal ions from aqueous solutions by activated carbon prepared from apricot stone," *Bioresour. Technol.* 96, 1518-1521.

Langmuir, I. (1916). "The constitution and fundamental properties of solids and liquids," *J. Am. Chem. Soc.* 38, 2221-2295.

Mall, I. D., Srivastava, V. C., Kumar, G. V. A., and Mishra, I. M. (2006). "Characterization and utilization of mesoporous fertilizer plant waste carbon for adsorptive removal of dyes from aqueous solution," *Colloid Surf A.* 278, 175-187.

Malkoc, E., Nuhoglu, Y., and Abali, Y. (2006). "Cr(VI) adsorption by waste acorn *Quercus ithaburensis* in fixed beds: Prediction of breakthrough curves," *Chem. Eng. J.* 119, 61-68.

Modher, A. H, Salleh, A., and Milow, P. (2009). "Characterization of the adsorption of the lead (II) by the nonliving biomass *Spirogyra neglecta* (Hasall) Kutzing," *Am. J. Biochem. & Biotech.* 6(1), 1-10.

Padmesh, T. V. N., Vijayaraghavan, K., Sekaran, G., and Velan, M. (2006). "Biosorption of Acid Blue 15 using fresh water macroalga *Azolla filiculoides*: Batch and column studies," *Dyes and Pigments* 71, 77-82.

Pan, X. L., Wang, J. L., and Zhang, D. Y. (2005). "Biosorption of Pb (II) by *Pleurotus ostreatus* immobilized in calcium alginate gel," *Process Biochem.* 40(8), 2799-2803.

Pruksathorn, P., and Vitidsant, T. (2009). "Production of pure ethanol from azeotropic solution by pressure swing adsorption," *Am. J. Engg. & Applied Sci.* 2(1), 1-7.

Salman, J. M., and Hameed, B. H. (2010). "Effect of preparation conditions of oil palm fronds activated carbon on adsorption of bentazon from aqueous solutions," *J. Hazard. Mater.* 175, 133-137.

Sarin, V., Singh, T. S., and Pant, K. K. (2006). "Thermodynamic and breakthrough column studies for the selective sorption of chromium from industrial effluent on activated eucalyptus bark," *Bioresour. Technol*. 97, 1986-1993.

Sekar, M., Sakthi, V., and Rengaraj, S. (2004). "Kinetics and equilibrium adsorption study of Pb(II) onto activated carbon prepared from coconut shell," *J. Colloid Interface Sci*. 279, 307-313.

Srivastava, P., and Hasan, S. H. (2011). "Biomass of *Mucor heimalis* for the biosorption of cadmium from aqueous solutions: Equilibrium and kinetices study," *Bioresources* 6(4), 3656-3675.

Taty-Costodes, V. C., Fauduet, H., Porte, C., and Ho, Y. S. (2005). "Removal of lead (II) ions from synthetic and real effluents using immobilized *Pinus sylvestris* sawdust adsorption on a fixed-bed column," *J. Hazard. Mater.* 123, 135-144.

Temkin, M. I., and Pyzhev, V. (1940). "Kinetics of ammonia synthesis on promoted iron catalyst," *Acta Physiochimica. USSR* 12, 327-356.

Thomas, H. C. (1944). "Heterogeneous Ion exchange in a flowing system,"*J. Am. Chem. Soc.* 66, 1466-1664.

Tofan, L., Paduraru, C., Irina, V., and Toma, O. (2011). "Waste of rapeseed from biodiesel production as a potential biosorbent for heavy metal ions," *BioResources* 6(4), 3727-3741.

Wong, K. K., Lee, C. K., Low, K. S., and Haron, M. J. (2003). "Removal of Cu and Pb by tartaric acid modified rice husk from aqueous solution,"*Chemosphere,* 50, 23-28.

Yoon, Y. N. and Nelson, J. H. (1984). "Application of gas adsorption kinetics. Part I. A theoretical model of respirator cartridge service time,"*J. Am. Ind. Hyg. Assoc.* 45, 509-516.

Zuorro, A., and Lavecchia, R. (2010). "Adsorption of Pb (II) on spent leaves of green and black tea,"*Am. J. Applied Sci*. 7, 53-59.

Zvinowanda, C. M., Okonkwo, J. O., Agyei, N. M., Van Staden, M., Jordaan, W., and Kharebe, V. (2010). "Removal of lead (II) from aqueous solutions by *Zea mays* tassel biosorption," *Am. J. Biochem. Biotechn*. 6(1), 1-10.

Article submitted: March 27, 2012; Peer review completed: May 15, 2012; Revised version received and accepted: May 17, 2012; Published: May 22, 2012.